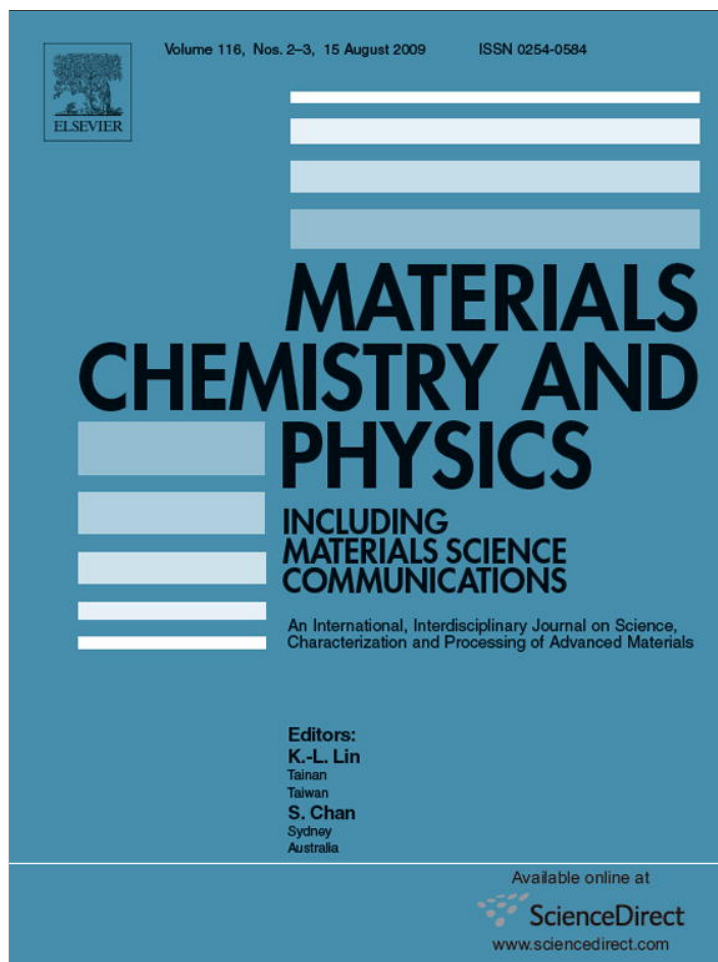


Provided for non-commercial research and education use.
Not for reproduction, distribution or commercial use.



This article appeared in a journal published by Elsevier. The attached copy is furnished to the author for internal non-commercial research and education use, including for instruction at the authors institution and sharing with colleagues.

Other uses, including reproduction and distribution, or selling or licensing copies, or posting to personal, institutional or third party websites are prohibited.

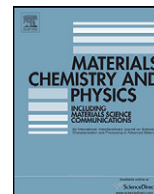
In most cases authors are permitted to post their version of the article (e.g. in Word or Tex form) to their personal website or institutional repository. Authors requiring further information regarding Elsevier's archiving and manuscript policies are encouraged to visit:

<http://www.elsevier.com/copyright>



Contents lists available at ScienceDirect

Materials Chemistry and Physics

journal homepage: www.elsevier.com/locate/matchemphys

Mesophase ordering and macroscopic morphology structuring of mesoporous TiO₂ film

M.J.Q. Yong^a, A.S.W. Wong^b, G.W. Ho^{c,*}^a Department of Chemical and biomolecular Engineering, National University of Singapore, 4 Engineering Drive 4, Singapore 117576, Singapore^b Institute of Materials Research and Engineering, 3 Research Link, Singapore 117602, Singapore^c Department of Electrical and Computer Engineering, National University of Singapore, 4 Engineering Drive 3, Singapore 117576, Singapore

ARTICLE INFO

Article history:

Received 8 January 2009

Received in revised form 3 April 2009

Accepted 18 April 2009

Keywords:

TiO₂

Self-assembly

Mesoporous

Sol-gel

ABSTRACT

An easy tuning of surface morphology of optically transparent TiO₂ film due to two different types of micellar packing; hexagonal structure consisting of close-packed cylindrical micelles and a cubic structure resulting from the close-packing of spherical micelles is demonstrated. By a calculable % volume fraction of block copolymer (BCP), the desired micelle crystal phase can be induced and the architectures of the polymer can be rationally tuned to effectively organize mesostructured composite solids with fairly large ordering length. P123 amphiphilic triblock copolymer PEO–PPO–PEO (EO)₂₀(PO)₇₀(EO)₂₀ is used as structure-directing agents for the highly organized metal oxide framework employing the evaporation induced self-assembled (EISA) route. The mesoporous structures have a narrow pore size distributions diameter of ~10 nm, wall thickness of ~5 nm and are well-crystallized with anatase phase.

© 2009 Elsevier B.V. All rights reserved.

1. Introduction

In order to make it feasible for the vast applications of TiO₂ for photocatalysts [1,2], gas sensors [3], photovoltaic cells [4–6] and rechargeable lithium batteries [7–10], it is essential to be able to tune and tailor specific mesoporous structures of thin films other than their porosity and thickness since they determine the specific surface area and charge carrier transport path of the material. The precise control of morphology and orientation of mesoporous thin films can be induced by self-assembled BCP into well-ordered periodic porous materials [11]. The control of the orientation of BCP is challenging as the BCP nanodomains spontaneously self-assemble into the configuration that minimizes the total free energy of the system and is confined by the polymer–substrate and polymer–air interfaces which undergo both surface relaxation and reconstruction. The ability to tailor the nanoscopic morphology of an inorganic matrix by changing the BCP alignment is very important since the surface morphology can dominate the properties of the material [11]. Thus, there are two important key things that have to be taken note for practical applications. Firstly, thin films of BCP are to be well-ordered with good periodicity and secondly, the desired alignment of the pores either hexagonal or cubic structure has to be tunable. Several approaches have been devised to induce the perpendicular alignment. Russell et al. employed the use of annealing

in an external electric field of a high strength ~30 kV cm⁻¹ that overcomes the surface fields to induce cylindrical or lamellae orientation of BCP [12]. Other approaches that have been proposed include the use of 'neutral surface' of substrate and also solvent induced orientations [13–16]. The substrate neutrality aims to minimize the difference in interfacial tensions between each block and substrate by adjusting the surface energy of the substrate. The resulting film successfully adopts perpendicular orientation from the bottom interface or substrate toward the surface exposed to air.

In this work, we report an easy switching of surface morphology due to two different types of P123 micellar packing; hexagonal structure consisting of close-packed cylindrical micelles and a cubic structure resulting from the close-packing of spherical micelles. P123 amphiphilic triblock copolymer PEO–PPO–PEO (EO)₂₀(PO)₇₀(EO)₂₀ is employed in our work since it possesses a variety of morphologies which includes spherical, cylindrical and lamellar phase. By a calculable % volume fraction of BCP, the desired micelle crystal phase can be induced and the architectures of the polymer can be rationally tuned to effectively organize mesostructured composite solids with fairly large ordering length. Thus, it is possible to control the mesophase ordering and macroscopic morphology adopted by the system. This is noteworthy since reconstruction and alignment of various BCP films have been reported by others using thermal annealing, strong electric field and neutral surface approach which require longer processing time, more complex procedures and even the use of an external stimuli to modify the surface ordering.

* Corresponding author. Tel.: +65 65168121; fax: +65 67754710.

E-mail address: elehgw@nus.edu.sg (G.W. Ho).

2. Experimental

The chemicals used in the experiments are concentrated hydrochloric acid (HCl), titanium (IV) tetraethoxide (TEOT) 33–35%, Pluronic poly(ethylene oxide)–poly(propyleneoxide)–poly(ethylene oxide) tri-block copolymer (P123) and ethanol. 3.2 g of HCl, 4.3 g of TEOT, 1 g of Pluronic P123 and 20 g of ethanol are magnetically stirred for approximately 10 min. The mixture is then aged at 13 °C for 48 h in a chiller. Subsequently, glass substrates are dip coated with dipping and withdrawing speed of 60 mm min⁻¹. The samples are then aged at 13 °C for 48 h in a chiller and subsequently calcined at 450 °C with a heating rate of 1 °C min⁻¹ to remove BCP and densify the TiO₂.

The amount of Pluronic P123 is varied between 0.5 and 2.0 g to investigate its effect on the film morphology and pore density. Other experiments that were carried out include the variation of the amount of ethanol, withdrawal speed, calcination temperature and concentration of Pluronic P123. The withdrawing speed during dip coating is varied between 60 and 120 mm min⁻¹ and the amount of ethanol is varied between 10 and 20 g to investigate their effects on the thickness of the film; all other factors are kept constant as stated in procedure. The calcination temperature between 350 and 550 °C is being varied to investigate its effect on the thickness and crystallinity of the film.

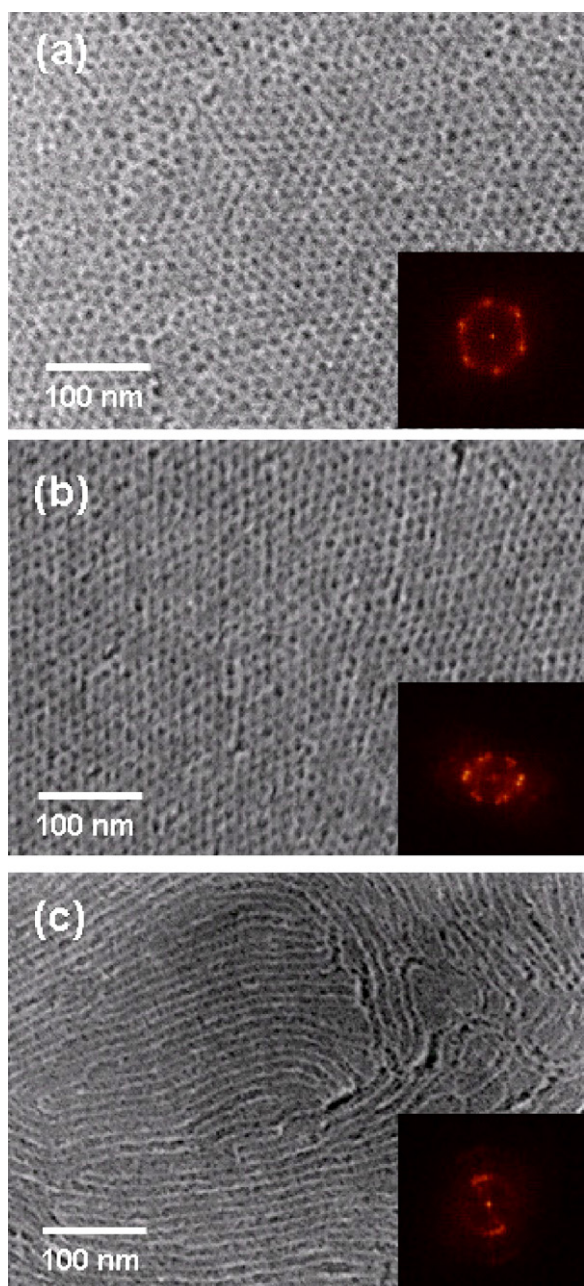


Fig. 1. SEM images of TiO₂ mesoporous film with (a) 1.0 g, (b) 1.5 g and (c) 2.0 g of BCP.

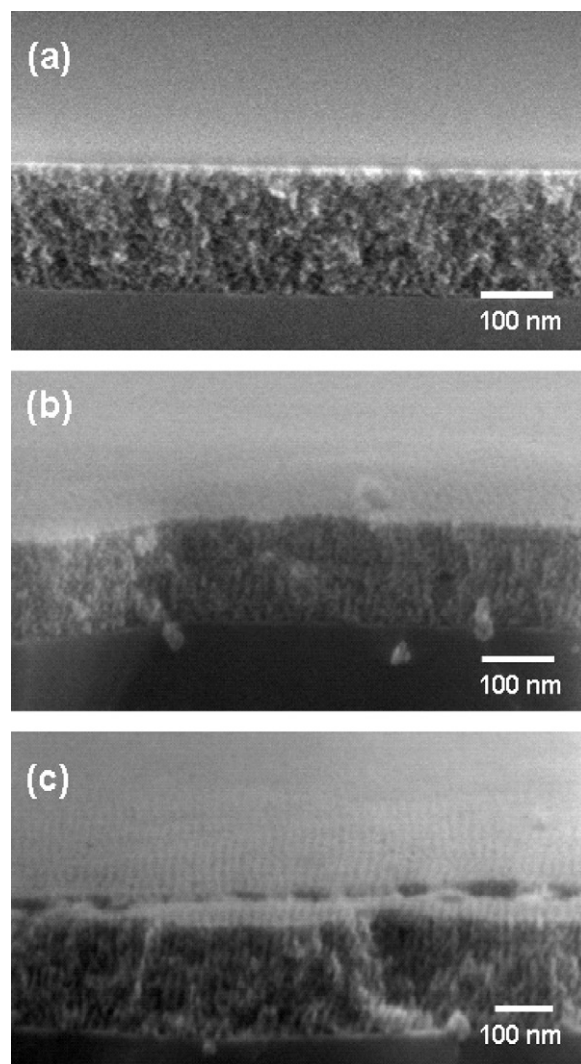


Fig. 2. Cross-sectional SEM images of TiO₂ mesoporous film with (a) 1.0 g, (b) 1.5 g and (c) 2.0 g of BCP.

The morphologies and film thickness were characterised using top and cross-sectional view scanning electron microscope (SEM, Jeol FEG JSM 6700 F, secondary electron imaging). X-ray photoelectron spectroscopy (XPS) was done using a VG ESCALAB MK2 equipped with an Mg K α X-ray source operating at 300 W. The crystallography and structures of the as-synthesized nanostructures were analysed using transmission electron microscope (TEM, Phillips FEG CM300) and X-ray diffractometer (XRD, Philip X-ray diffractometer equipped with a graphite monochromator Cu K α radiation $\lambda = 1.541 \text{ \AA}$). The transmittance spectrum was measured using a Shimadzu UV-3600 UV–vis double-beam spectrometer.

3. Results and discussion

The self-organization of TiO₂ nanoparticles is directly related to the BCP templating effect. P123 amphiphilic triblock copolymer is a nonionic surfactant and the driving force for the micelle forming is the result of the hydrophilicity between the polyethylene oxide (PEO) and polypropylene oxide (PPO) chains. Titanium dioxide hydrate has affinity binding to the P123 unit which then creates the self-assembled mesoporous structures. The fabrication can be obtained following the EISA route which is based on the evaporation of an organic solvent promoting 2D or 3D self-assembly of the surfactant and the simultaneous condensation of the inorganic oxide precursor. The formation of well-organized structures by EISA is observed when the evaporation is almost complete just as the surfactant is in close contact with oxide precursor. In this experi-

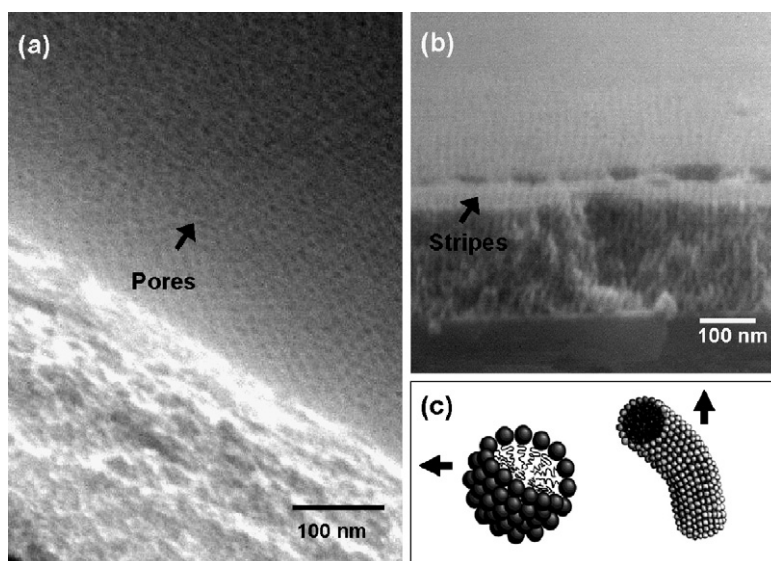


Fig. 3. High-magnification SEM images of (a) 1.0 g, (b) 2.0 g of BCP and (c) illustrations of spherical and cylindrical micelles.

mental procedure, Pluronic P123 acts as a structure-directing agent while concentrated HCl prevents rapid condensation of the TiO_2 precursor, TEOT. The aging temperature is controlled to be as low as 13°C so as to slow down the mesostructure formation process. The long aging process promotes full framework condensation to effectively allow self-assembly of nanostructures into ordered pores. As compared to the other physical template-assisted method, this EISA method is much simpler and able to reproducibly fabricate highly ordered mesoporous TiO_2 structure.

SEM images in Fig. 1 are samples synthesized with different amount of BCP. In general, when 0.5–1.0 g of P123 is used, well-structured pores are obtained. Fig. 1a shows the morphology of the dip coated film with 1.0 g of copolymer incorporated into the matrix. The mesoporous film shows a high-density of quasi-hexagonal pores of ~ 10 nm in diameter. The fast Fourier transform (FFT) image (Fig. 1a inset) shows six sharp first order peaks suggesting the almost perfect hexagonal order. The morphology can be easily tuned with appropriate amount of BCP as an increased in copolymer concentration to 1.5 g (Fig. 1b), short range of aligned pores are observed across the sample. FFT pattern (Fig. 1b inset) indicates a preferential orientation of the pores and the dimension of the pores remains ~ 10 nm. With further increase in copolymer concentration to 2.0 g, stripes of aligned pores become more prominent though small number of hexagonal pores is still randomly observed (Fig. 1c). The stripes are not completely random in orientation as they are self-aligned and assembled parallel to each other over a short range. FFT (Fig. 1b inset) shows two segmented rings suggesting preferred alignment of the stripes across the sample. The density of well-structured quasi-hexagonal pores drops as the amount of copolymer increased beyond a critical micelle concentration (CMC) to Ti ratio due to the occurrence of copolymer micelles fusion or aggregation which causes the formation of stripes or lamellae surface structuring. As the micelle crystal is formed the dispersed inorganic particles are constrained to the remaining interstitial spaces between the micelles, thereby occupies most of the volume space to form mesoporous structures.

The surface structuring of the TiO_2 film may be predicted simply by calculating the volume fraction of BCP (ϕ) in the nonvolatile components of the solution [17]. The formation of well-organized TiO_2 structures by EISA as mentioned occurs only when the evaporation of ethanol is complete just as the BCP is close in contact with oxide precursor, thus ethanol is not taken into account in the

calculation of the volume fraction. Considering only the BCP and inorganic precursor species, ϕ is defined as [17]:

$$\phi = \frac{V_{\text{BCP}}}{V_{\text{BCP}} + V_{\text{inorg}}} \quad (1)$$

where V_{BCP} and V_{inorg} is the volume of the block copolymer and the inorganic metal oxide constituent, respectively.

$$V_{\text{BCP}} = \frac{m_{\text{BCP}}}{\rho_{\text{BCP}}} \quad (2)$$

$$V_{\text{inorg}} = \frac{m_{\text{M(OH)}_4}}{\rho_{\text{M(OH)}_4}} + \frac{m_{\text{HCl}}}{\rho_{\text{HCl}}} \quad (3)$$

where m_{BCP} , $m_{\text{M(OH)}_4}$, m_{HCl} and ρ_{BCP} , $\rho_{\text{M(OH)}_4}$, ρ_{HCl} are mass and density of BCP, metal hydroxides and HCl, respectively.

Since the nature of the sol-gel precursors when the TiO_2 mesoporous structure is formed cannot be precisely determined, the calculation of V_{inorg} is based on estimation [17]. The sol-gel precursors are considered to be fully hydrolyzed, uncondensed metal hydroxides. In the case of TiO_2 , the volume of hydrochloric acid is included in the calculation of V_{inorg} , because it is complexed with the titania species and hence is incorporated to a significant extent into the films [17].

With a calculable change in volume fraction of the BCP, the predictable surface structuring of TiO_2 film with micelle crystal phase (spherical or cylindrical micelles) can be predominantly induced. The calculated % volume fractions are as tabulated in Table 1. At a concentration of <31% volume fraction, P123 exhibit spherical micelles (cubic packing) and at 37% volume fraction, the polymer undergoes a transition from the soft crystal of spherical micelles into cylindrical micelles (hexagonal packing). The structure expected corresponds to the water-surfactant phase diagram which has a bidimensional hexagonal structure consisting of close-

Table 1

Summary of the effect of % volume fraction of P123 on the pore density and the mesophase ordering and macroscopic morphology.

P123 mass (g)	Micelle phase	Vol. fraction (%)
0.5	Spherical	13
1.0	Spherical	23
1.5	Spherical	31
2.0	Cylindrical	37

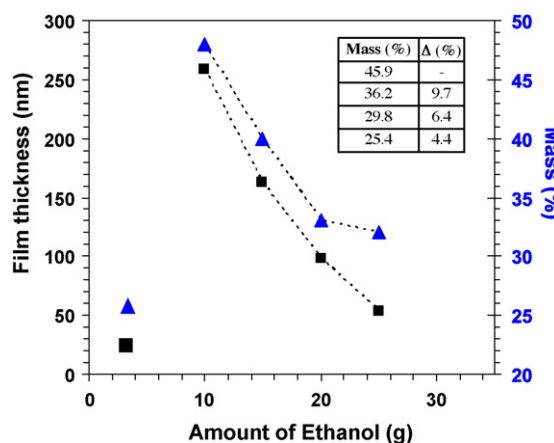


Fig. 4. Plot of film thickness and mass percentage vs. the amount of ethanol. Inset shows a table of relative percentage mass composition change.

packed cylindrical micelles or a cubic structure resulting from the close-packing of spherical micelles [18].

High-resolution SEM images are taken in order to show evidences of the various film structures although it proves to be very difficult to obtain clear images. The transition from the spherical micelles (cubic packing) to the cylindrical micelles (hexagonal packing) is evident from the cross-sectional SEM images as shown in Fig. 2a–c which corresponds to Fig. 1a–c. Higher magnification cross-sectional SEM of Fig. 3a shows well-defined ~ 10 nm diameter pores associated to closely packed spherical micelles whereby cubic packing mesostructures is resulted. The cubic packing did not induce perpendicular orientation as can be seen from the top to the bottom substrate (Fig. 3a). As the BCP volume fraction is increased

to 2.0 g, the cross-sectional morphology (Fig. 3b) shows an apparent cylindrical micelles as evident from the perpendicular alignment of the metal oxide. The perpendicular orientation did not propagate all the way from the top of the film–air interface to the bottom of the film–substrate interface. The perpendicularly oriented domains are mainly observed in the upper part of the film and partially propagate down to the bottom part of the film. There is a transition of the TiO₂ mesostructured film from a non-perpendicular orientation cubic packing (Fig. 2a) to intermediate (Fig. 2b) and finally partial perpendicular hexagonal packing (Fig. 2c). It is noteworthy that the possibility of switching the surface morphology into two different types of alignments is due to micellar packing (Fig. 3c); cubic structure resulting from the close-packed spherical micelles and hexagonal structure consisting of close-packed cylindrical micelles.

Following this, ways to tune the thickness of the TiO₂ film via withdrawal speed, calcination temperature and amount of ethanol are explored. Various number of dip coatings on glass substrates and heat treatment at 450 °C were carried out. The films were observed to be uniformly coated and crack-free using an optical microscope. The transmittance measurements were performed with a plain glass substrate as reference in the double-beam spectrometer. After the annealing of the TiO₂ film at 350 °C, the transmission decreases from 93 to 90% which may be resulted from the scattering of light due to the crystallization and grain aggregation of TiO₂ nanocrystallites. However, there is no significant change in the optical transmission between the samples with an annealing temperature of 350 and 450 °C. In additional, surface morphology variation does not induce any significant change in transmission across the wavelength measured. In general, the films were transparent and the average percentage of light transmitted through the TiO₂ films in the visible light range was approximately 90%.

The effect of various withdrawing speed, calcination temperature and ethanol concentration on film thickness that was studied

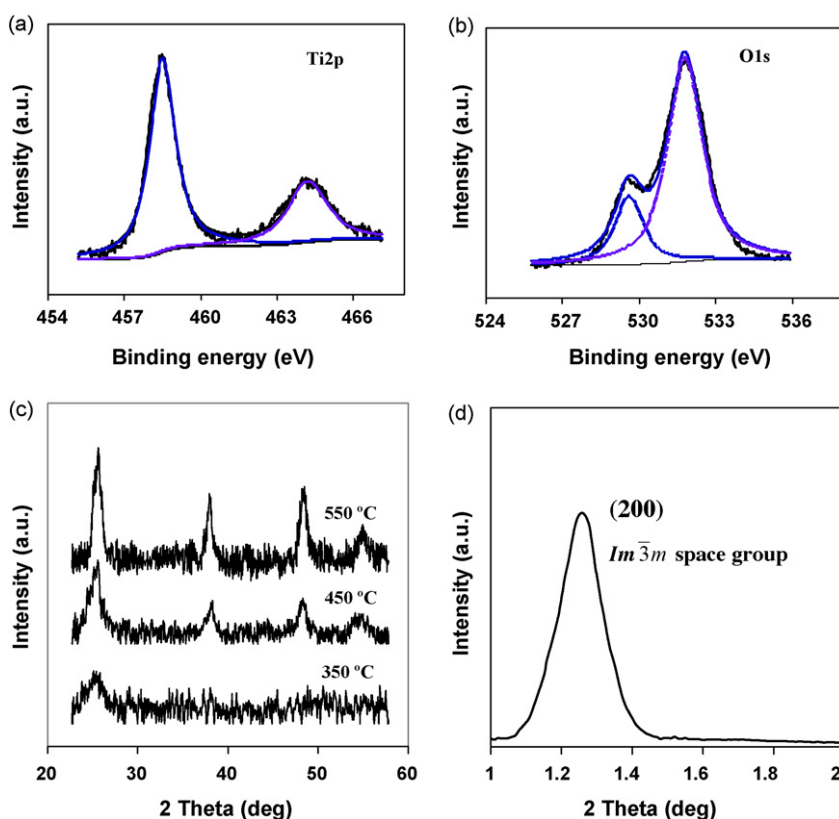


Fig. 5. (a) Ti 2p and (b) O 1s XPS spectrum of the mesoporous film. (c) XRD spectra of TiO₂ film heat treated at various calcination temperatures. (d) Small angle XRD spectrum of TiO₂ film with 1.0 g P123.

Table 2

Effect of withdrawing speed, temperature and ethanol concentration on the dip-coated film thickness.

Sample	Ethanol conc. (g)	Withdrawing speed (mm min ⁻¹)	Temp. (°C)	Thickness (nm)
M1	10	60	450	280
M2	15	60	450	200
M3	20	60	450	130
M4	20	120	350	180
M5	20	120	450	230
M6	25	60	450	120

are shown in Table 2. From Table 2 (M3 and M5), it can be seen that as the withdrawing speed is increased from 60 to 120 mm min⁻¹, the thickness of the TiO₂ mesoporous film increases from 130 to 230 nm, approximately 1.8 times the original thickness. On the other hand, the effect of calcination temperature on film thickness can be observed by comparing M4 and M5 samples. As the temperature is decreased from 450 to 350 °C keeping other parameters constant, it is observed that the film thickness decreased with calcination temperature. Higher temperature leads to film shrinkage as a result of relative higher condensation and partial crystallization of titania network. As for the effect of amount of ethanol with the film thickness, it is observed that as the amount of ethanol increases from 10 to 20 g (M1, M2 and M3), the thickness of the film is observed to decrease rather quickly from 280 to 130 nm. From Fig. 4, a linear relationship between the film thickness and the amount of ethanol used is noted. However, when the amount of ethanol is further increased to 25 g (M6), a minimal change in thickness is observed, which may suggest that there is a limitation to the minimum thickness one can tune with the ethanol concentration. This can probably be explained by the changes in the percentage mass composition of constituents left in the reaction mixture after the evaporation of ethanol. The percentage mass composition difference between M1 and M2 is 9.7% while M2 and M3 is 6.4% (Fig. 4 inset). However, when the amount of ethanol is increased from 20 to 25 g (M3 and M6), the percentage change drops to 4.4%. The relatively smaller percentage change in mass composition for higher ethanol concentration sample (M6) resulted in a minimal change in the thickness of the film. In general, the fine film thickness can be varied between ~100 and 300 nm by controlling the withdrawal speed, calcination temperature and the amount of ethanol used to dilute the precursor mixture.

XPS analysis was used to determine the surface properties of mesoporous film that was prepared. The Ti 2p peak positions for the as-prepared mesoporous film are at 458.6 and 464.2 eV, which can be assigned to the core levels of Ti⁴⁺ 2p_{3/2} and Ti⁴⁺ 2p_{1/2}, respectively (Fig. 5a) [19]. The peak fitted O 1s peaks (Fig. 5b) were composed of two chemical states, one is the lattice oxygen Ti–O–Ti (529.6 eV) and the other is the chemical absorbed OH (531.5 eV) [18]. The ratio of lattice O²⁻ to hydroxyl groups is ~2.15 indicating the existence of large amounts of OH groups on the surface of the as-prepared TiO₂ mesoporous structure. XRD analysis was used to investigate the crystallinity of the TiO₂ at different calcination temperatures. Fig. 5c shows XRD spectrum of TiO₂ mesoporous films which have been annealed at 350, 450 and 550 °C. It is observed that diffraction peaks at 25.58, 38.3, 48.32 and 54.76° are distinctive for samples annealed at 450 and 550 °C, and were identified to be anatase TiO₂ [20]. Crystallinity of the TiO₂ mesoporous film is observed to improve with calcination temperature as the intensity of (101) anatase peak increases with temperature. However, it is noted that the improvement of crystallinity is accompanied by fusing, particle size growth as the diffraction peak is observed to become narrower as the calcination temperature increased. Fig. 5d shows a small angle XRD spectrum of TiO₂ sample with 1.0 g P123 (Fig. 1a). The presence of one diffraction peak indicates that the film

has short range order. The peak is indexed as the (200) reflection of *Im3m* space group of cubic mesostructured film.

Fig. 6a shows the TEM image of TiO₂ film synthesized using 1.0 g P123 which shows its cubic mesostructures. An average pore size of ~10 nm and wall structure of ~3–7 nm is determined. High-resolution TEM of Fig. 6b shows randomly oriented ~3–5 nm diameter TiO₂ nanocrystallites. Fig. 6c shows the plan-view TEM image of the hexagonal mesostructured TiO₂ film which shows the

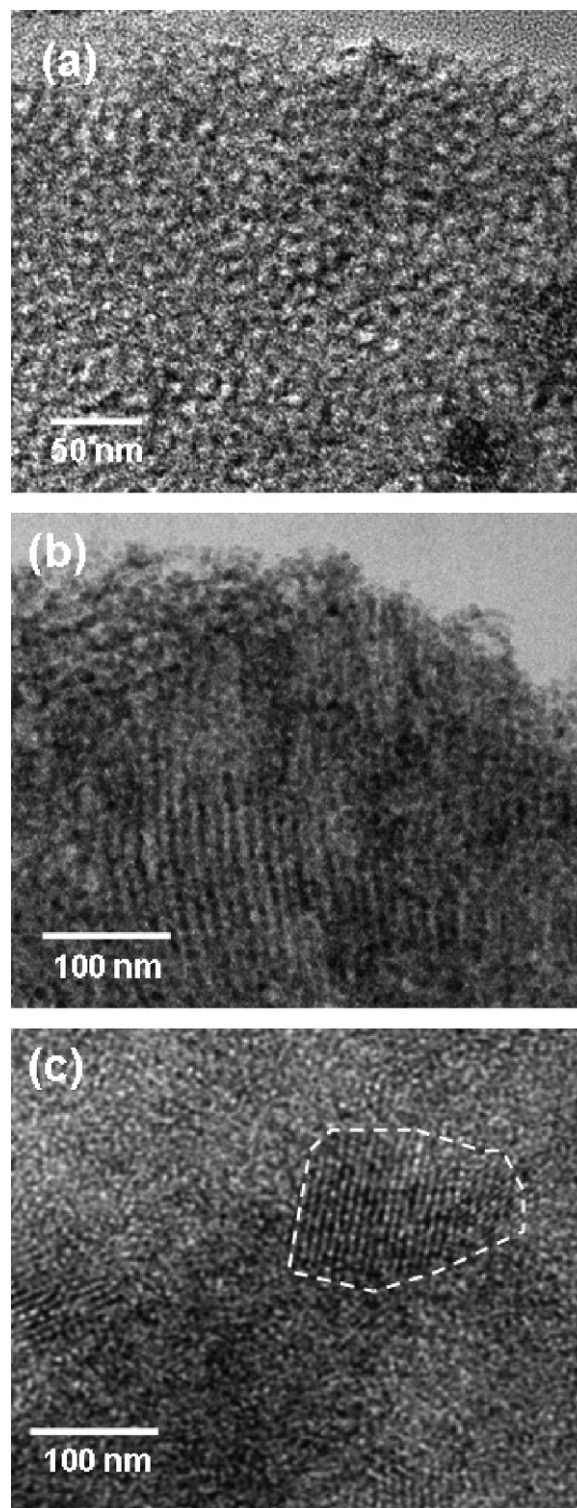


Fig. 6. TEM image of calcined TiO₂ mesoporous structures with (a) cubic, (b) hexagonal packing film and (c) high-resolution image of TiO₂ nanocrystallites.

cylinder-forming BCP with pore diameter of ~ 10 nm. The films are not well-ordered throughout the films thickness.

4. Conclusion

We have shown that it is possible to control the mesophase ordering and macroscopic morphology adopted by the crack-free optically transparent TiO_2 system. An easy switching of surface morphology of TiO_2 film due to two different types of micellar packing; hexagonal structure consisting of close-packed cylindrical micelles and a cubic structure resulting from the close-packing of spherical micelles is demonstrated. At a concentration of $<31\%$ volume fraction, P123 exhibit spherical micelles and at 37% volume fraction, the polymer undergoes a transition from the soft crystal of spherical micelles into cylindrical micelles. The effect of the dip-coating withdrawal speed, calcination temperature and ethanol concentration can be used to tune the thickness of the film deposited. The mesoporous structures have a narrow pore size distributions diameter of ~ 10 nm and framework structure of ~ 5 nm. The resultant mesoporous structures are well-crystallized with anatase phase. A good control of thickness and morphology is important since they determine the specific surface area and charge carrier transport path which directly influence the application of photovoltaic, photocatalyst, battery and gas sensing materials.

Acknowledgments

This work is supported by the National University of Singapore (NUS) grants R-533 000 002 123 and R-533 000 003 112 and Applied materials. The authors would like to thank Mr. Wong How Kwong and the usage of the Surface Science Lab facilities.

References

- [1] N. Venkatachalam, M. Palanichamy, V. Murugesan, *Mater. Chem. Phys.* 104 (2007) 454.
- [2] S.Z. Chu, S. Inoue, K. Wada, D. Li, H. Haneda, S. Awatsu, *J. Phys. Chem. B* 107 (2003) 6586.
- [3] O.K. Varghese, D.W. Gong, M. Paulose, K.G. Ong, E.C. Dickey, C.A. Grimes, *Adv. Mater.* 15 (2003) 624.
- [4] P. Ravirajan, S.A. Haque, J.R. Durrant, D. Poplavskyy, D.D.C. Bradley, J. Nelson, *J. Appl. Phys.* 95 (2004) 1473.
- [5] A.C. Arango, S.A. Carter, P.J. Brock, *Appl. Phys. Lett.* 74 (1999) 1698.
- [6] A.C. Arango, L.R. Johnson, V.N. Bliznyuk, Z. Schlesinger, S.A. Carter, H.H. Horhold, *Adv. Mater.* 12 (2000) 1689.
- [7] O. Wilhelm, S.E. Pratsinis, E. de Chambrier, M. Crouzet, I. Exnar, *J. Power Sources* 134 (2004) 197.
- [8] L. Kavan, J. Rathousky, M. Grätzel, V. Shklover, A. Zukal, *J. Phys. Chem. B* 104 (2000) 12 012.
- [9] L. Kavan, M. Kalbac, M. Zukalova, I. Exnar, V. Lorenzen, R. Nesper, M. Grätzel, *Chem. Mater.* 16 (2004) 477.
- [10] L. Kavan, J. Rathousky, M. Grätzel, V. Shklover, A. Zukal, *Micropor. Mesopor. Mater.* 44 (2001) 653.
- [11] A. Sidorenko, I. Tokarev, S. Minko, M. Stamm, *J. Am. Chem. Soc.* 125 (2003) 12211.
- [12] T.L. Morkved, M. Lu, A.M. Urbas, E.E. Elrich, H.M. Jaeger, P. Mansky, T.P. Russell, *Science* 273 (1996) 931.
- [13] E. Huang, T.P. Russell, C. Harrison, P.M. Chaikin, R.A. Register, C.J. Hawker, J. Mays, *Macromolecules* 31 (1998) 7641.
- [14] G. Kim, M. Libera, *Macromolecules* 31 (1998) 2569.
- [15] G. Kim, M. Libera, *Macromolecules* 31 (1998) 2670.
- [16] H. Elbs, C. Drummer, V. Abetz, G. Krausch, *Macromolecules* 35 (2002) 5570.
- [17] P.C.A. Alberius, K.L. Frindell, R.C. Hayward, E.J. Kramer, G.D. Stucky, B.F. Chmelka, *Chem. Mater.* 14 (2002) 3284.
- [18] S.S. Soni, G. Brotons, M. Bellour, T. Narayanan, A. Gibaud, *J. Phys. Chem. B* 110 (2006) 15157.
- [19] B.S. Liu, L.P. Wen, X. Zhao, *J. Sol. Energy Mater. Sol. Cells* 92 (2008) 1.
- [20] J. Yang, S. Mei, J.M.F. Ferreira, *J. Mater. Res.* 17 (2002) 21972200.